Fragility and anomalous susceptibility of weakly interacting networks

Giacomo Rapisardi,[1,*] Alex Arenas,[2] Guido Caldarelli,[1,3,4] and Giulio Cimini[1,3]
[1]*IMT School for Advanced Studies, 55100 Lucca, Italy*
[2]*Departament d'Enginyeria Informàtica i Matemàtiques, Universitat Rovira i Virgili, 43007 Tarragona, Spain*
[3]*Istituto dei Sistemi Complessi (CNR) UoS Sapienza, 00185 Rome, Italy*
[4]*European Centre for Living Technology, Università di Venezia "Ca' Foscari," 30124 Venice, Italy*

(Received 10 December 2018; published 3 April 2019)

Percolation is a fundamental concept that has brought new understanding of the robustness properties of complex systems. Here we consider percolation on weakly interacting networks, that is, network layers coupled together by much fewer interlinks than the connections within each layer. For these kinds of structures, both continuous and abrupt phase transitions are observed in the size of the giant component. The continuous (second-order) transition corresponds to the formation of a giant cluster inside one layer and has a well-defined percolation threshold. The abrupt transition instead corresponds to the merger of coexisting giant clusters among different layers and is characterized by a remarkable uncertainty in the percolation threshold, which in turns causes an anomalous behavior of the observed susceptibility. We develop a simple mathematical model able to describe this phenomenon, using a susceptibility measure that defines the range where the abrupt transition is more likely to occur. Finite-size scaling analysis in the abrupt region supports the hypothesis of a genuine first-order phase transition.

DOI: 10.1103/PhysRevE.99.042302

Percolation theory is a very successful framework for understanding a broad range of critical phenomena taking place on networks, such as robustness to failures or attacks and spreading of diseases or information, and for unveiling the common principles underlying these processes [1,2]. In this context, multilayer networks have been shown to exhibit critical percolation properties which are different from what is observed for a single isolated network, namely, a single continuous phase transition [3,4] whose properties depend on the kind of process [5] and on the network features [6,7]. Indeed, the presence of interconnections between the network layers can give rise to supercritical phenomena such as abrupt or multiple phase transitions. Discontinuous percolation transitions have been extensively reported in the case of interdependent networks, that is, two (or more) networks whose nodes are interconnected by dependency links, such that the removal of a node in a network causes the instantaneous removal of the dependent nodes in the other networks (see, for instance, Refs. [8–10]). Our focus here is instead on interacting networks (or network of networks), in which the connections between the network layers are ordinary links that thus take part in the percolation process. A system of this kind is therefore equivalent to a single modular network, characterized by a percolation threshold that is typically lower than in homogeneous networks, with a giant cluster appearing for a smaller total number of links [11]. A case of particular interest arises when the interaction between the network layers is weak, meaning that there is a sufficiently small number of interlinks between network layers, so that the removal of a few of them can easily separate the network layers into isolated modules [12,13]. This setup is common for neural systems and therefore of major relevance to understand the resilience of neural processing [14]. Weakly interacting networks are characterized by a mixed percolation phase, in which only one or some of the network layers do percolate [15,16]. In particular, Colomer-de-Simón and Boguñá [17] identified multiple percolation transitions when the coupling between the different layers vanishes in the thermodynamic limit. In order to account for the emergence of coexisting percolating clusters, Faqeeh *et al.* [18] developed a modular message passing approach. In any event, the appearance of these coexisting clusters in weakly interacting networks is a fundamental source of error for percolation theory. Here we present a simple mathematical framework that allows estimating the most likely critical threshold at which the merging of coexisting clusters occurs in weakly interacting networks. Moreover, we characterize the percolation process in terms of a powder keg: due to the scarcity of the interlinks, the aggregation of the coexisting giant clusters is delayed, therefore giving rise to an abrupt percolation transition.

To illustrate the percolation properties of weakly interacting networks, we consider as in Fig. 1 two layers A (with N_A nodes and average degree k_A) and B (with N_B nodes and average degree k_B), that are interconnected by a small number I of links ($I \ll \min\{N_A k_A, N_B k_B\}$). The bond percolation process consists in retaining each link of the system with occupation probability f and otherwise removing it. To simulate the process, we use the method proposed by Newman and Ziff [19]: for each realization, we start from a system configuration with no connections and then sequentially add links in a random order. f is thus the fraction of links added to the system. In such a situation, we observe large jumps for the order parameter S, that is, the size of the giant cluster

*giacomo.rapisardi@imtlucca.it

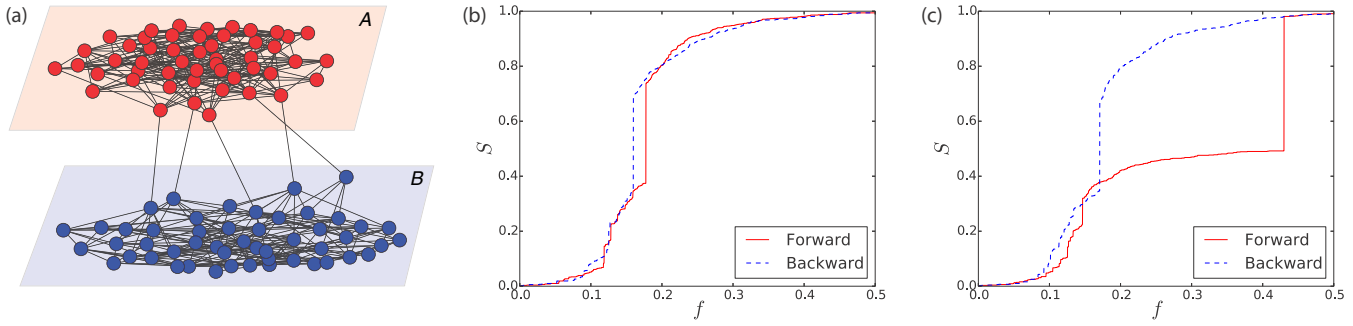

FIG. 1. Single realizations of bond percolation on a weakly interacting network. (a) Pictorial representation of two weakly interacting networks A and B, in which the interconnection links I are much fewer than the intralayer links. (b), (c) Two different instances of the percolation process on an interacting network composed of two Erdős-Rényi layers ($N = 500$ nodes and average degree $k = 10$ each) connected by $I = 5$ interconnection links. Each realization is obtained as follows. Starting from an empty network, links are first randomly added (*forward*) up to half the total number of links, and then randomly removed (*backward*) until the network is empty again. Discontinuous jumps in the relative size of the giant component S appear at four remarkably different values of the occupation probability f, due to the statistical fluctuations affecting the percolation threshold.

spanning both layers. These jumps can be understood as resulting from the addition of one of the I interlinks *after* the formation of the two giant clusters S_A and S_B of layers A and B, respectively. Indeed, differently from what happens for standard percolation, when such an interlink is about to be added the two giant clusters already contain a number of nodes that is proportional to the system size. According to the definition of Friedman *et al.* [20], this configuration corresponds to a *powder keg*, which is "ignited" as soon as that interconnection is added, causing a discontinuous percolation transition. Note that if a system is initialized as a powder keg, then even a random link addition rule causes a discontinuous transition: as in our case, the formation of the giant cluster spanning both layers is not hindered by specific link selection rules [21–25] but is naturally delayed by the structure of the interconnections itself. However, the absence of any particular link selection criteria causes a large uncertainty for the percolation threshold: discontinuous jumps in S are observed for very different values of the link occupation probability among independent realizations of the process (see Fig. 1).

In order to gain a more quantitative insight into the described phenomenology, we start by defining the probability P_I that at least one of the I interconnections is added and actually connects the two giant clusters S_A and S_B [18]:

$$P_I = 1 - \left[1 - \left(\frac{N}{N_A}S_A\right)\left(\frac{N}{N_B}S_B\right)f\right]^I = 1 - \left[1 - \frac{N}{\mu}S_A S_B f\right]^I, \tag{1}$$

where $N = N_A + N_B$ is the total number of nodes, the normalization coefficients before S_A and S_B, respectively, denote their maximum size N_A/N and N_B/N, and $\mu = \frac{N_A N_B}{N_A + N_B}$ is the *reduced* number of nodes (equivalent to the concept of reduced mass for the classical two-body problem). Without loss of generality, we set the percolating thresholds f_A and f_B of the individual layers A and B, respectively, such that $f_A < f_B$ (the degenerate case $f_A = f_B$ is reported below and discussed in the Appendix). This implies that on average and for layers of the same nature we have $S_A > S_B$ for any given value of f such that both clusters exist. Hence, for $f > f_B$, the percolation cluster S of the whole system either is that of layer A if S_A and S_B are not connected or abruptly jumps to $S_A + S_B$ provided that S_A and S_B are connected, which happens with probability P_I. In formulas,

$$S = \begin{cases} S_A + S_B & \text{with probability } P_I \\ S_A & \text{otherwise} \end{cases}. \tag{2}$$

Overall, we have a first continuous transition at $f_1 = f_A$ (the standard percolation transition when layer A percolates) and a second discontinuous transition at f_2 when layer B percolates and at least one active interconnection is established between the two layers. Yet, because of the dichotomy characterizing the outcome of the process for $f \simeq f_2$, the average value $\langle S\rangle = S_A + S_B P_I$ is not representative at all of what happens in the system. We thus study the behavior of the susceptibility $\chi = N\mathrm{Var}(S)/\langle S\rangle$ [17]. For $f > f_B$ each layer has its own percolating cluster, and thus the only contribution to χ comes from the Bernoulli trial described by Eq. (2):

$$\chi_D = N\frac{S_B^2 P_I(1 - P_I)}{S_A + S_B P_I}. \tag{3}$$

Note that χ_D gives a nonvanishing contribution to the total susceptibility χ only in the weakly interacting regime, that is, when the Bernoulli trial of Eq. (2) is not trivial. Indeed, Eq. (1) says that for $I \to 0$ (as for the case of disconnected layers) we have $P_I \to 0$, and when I is very large (as is the case of strongly connected layers; see the Appendix) we have $P_I \to 1$. In both cases $\chi_D \to 0$. For fixed I, however, χ_D achieves its maximum for the value of f which maximizes the uncertainty of the Bernoulli trial, at which the discontinuous jump of S is more likely to occur. We thus identify f_2 with the value for f which maximizes χ_D.

These simple mathematical arguments are indeed able to capture the behavior of the susceptibility in both real and model networks. We first consider in Fig. 2 the duplex (two-layer multiplex) formed by a pair of coupled air transportation networks, where each layer consists of the airports (nodes) and flight routes (links) operated by a given company, and the interlinks correspond to the airports served by both companies. We see that the susceptibility of the two individual layers χ_C cannot capture the observed behavior of χ computed

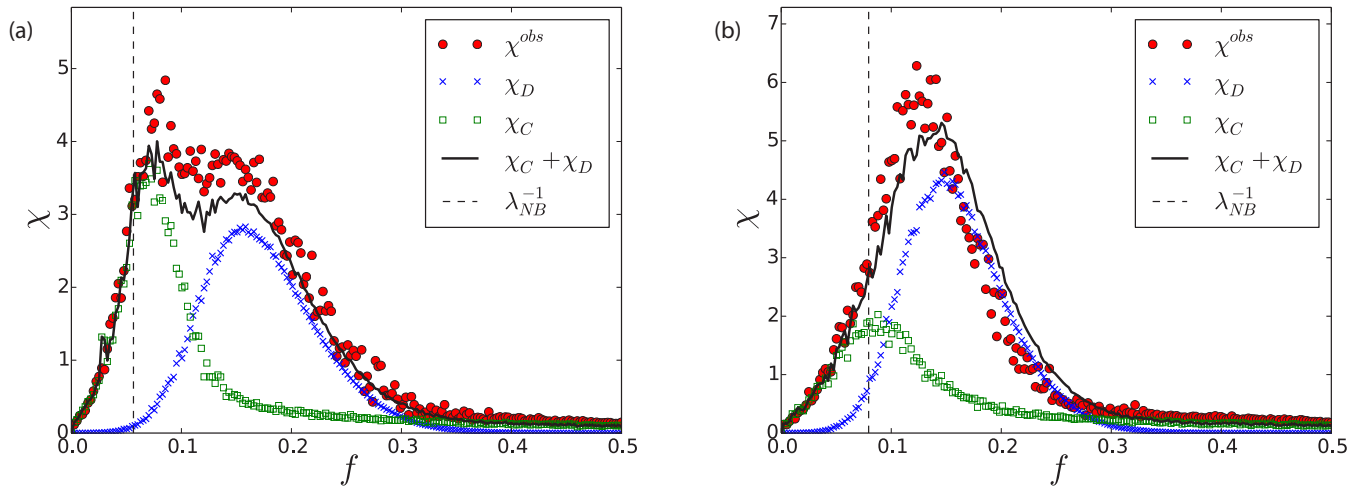

FIG. 2. Susceptibility of air transportation networks. We consider the duplex formed by the transportation network Lufthansa (LH)–Ryainair (FR) in panel (a) and Lufthansa (LH)–Easyjet (U2) in panel (b) [26], in which each layer is made up of airports (nodes) and flight routes (links) operated by a company. The layers are characterized by $N_{\mathrm{LH}} = 106$ and $\langle k\rangle_{\mathrm{LH}} = 4.604$, $N_{\mathrm{FR}} = 128$ and $\langle k\rangle_{\mathrm{FR}} = 9.391$, and $N_{U2} = 99$ and $\langle k\rangle_{U2} = 6.202$. The interconnection links in each case correspond to the airports in which both companies operate: we have $I_{\mathrm{LH-FR}} = 36$ and $I_{\mathrm{LH}-U2} = 51$. Full red dots denote numerical values of χ computed from 400 realizations of the bond percolation process. χ_D (blue crosses) is given by Eq. (3), and χ_C (green squares) is the susceptibility of the corresponding noninteracting system. λ_{NB} is the leading eigenvalue of the Hashimoto nonbacktracking matrix of the network, whose inverse is a good approximation for the percolation threshold of sparse networks [27].

numerically. The difference between χ and χ_C is instead very well represented by χ_D.

A more precise assessment of our methodology is given by considering two Erdős-Rényi weakly interacting networks with the same number of nodes $N_A = N_B$ and average degrees k_A and k_B. In this case it is possible to derive an analytic approximation for f_2, since S_A and S_B have a known analytic form in the thermodynamic limit. We get (see the Appendix for details)

$$f_2 = \frac{1 - 2^{-1/I}}{1 - \exp[-k_B(1 - 2^{-1/I})]}. \tag{4}$$

The specific case $k_A = k_B = k$ leads to a more accurate transcendental equation (see the Appendix):

$$f_2 = \frac{1 - (2-\sqrt{2})^{1/I}}{(1 - \exp\{-k\sqrt{f_2[1 - (2-\sqrt{2})^{1/I}]}\})^2}, \tag{5}$$

which can be easily solved numerically. As shown in Fig. 3, in the case of two weakly interacting Erdős-Rényi networks with different average degrees, the numerical evaluation of χ_D by means of Eq. (3) fits very well the observed anomalous susceptibility, and the numerical solution of Eq. (4) gives with good approximation the position of the maximum of χ. In the degenerate case $k_A = k_B$, Eq. (5) provides an even better approximation for the maximum of χ. Analyzing single realizations of the percolation process, we confirm that f_2 marks the region in which S is subject to discontinuous jumps. However, this discontinuous behavior is lost by averaging the results of the percolation process over many realizations, for which S becomes $\langle S\rangle = S_A + P_I S_B$, which simply fails to represent the outcome of the process.

We conclude our study with a finite-size scaling analysis carried out for the cases of two coupled Erdős-Rényi layers and two coupled Barabási-Albert layers with different average connectivities. For each of these settings we consider layers with size $N_{A,B}$ equal to 100, 500, 2500, and 12 500. According to standard percolation theory, the maximum of the susceptibility diverges around the critical value f_c following the power law $\chi(f_c) \sim N^{1-\beta/\nu}$, while for the relative size of the giant component we have $S(f_c) \sim N^{-\beta/\nu}$ [5,17]. Our analysis, reported in Fig. 4, shows that the scaling properties around f_1 and f_2 are significantly different. While $S(f_1)$ and $\chi(f_1)$ exhibit the usual power law scaling typical of second-order phase transitions (with different exponents according to the two different topologies of the network layers), $S(f_2)$ does not scale with N in both examples, which implies $\beta/\nu = 0$ and in turn $\chi(f_2) \sim N$. These particular scaling properties, that is, the failure of finite-size scaling relations and the extensive character of the susceptibility, are a clear trademark of a first-order phase transition [28].

To sum up, in this work we have studied the bond percolation properties of weakly interacting networks. This class of systems encompasses the important cases of multilayer or modular networks with very sparse connections within the layers or modules. We reported the existence of discontinuous jumps in the relative size of the giant component S, happening since the percolating cluster of the sparser layer can give either a full or zero contribution to the giant cluster of the whole system. Furthermore we observed that in this case the abrupt transition does not have a definite threshold but can occur for a wide range of values of the bond occupation probability. This causes an anomalous behavior of the susceptibility, which we captured using simple probabilistic arguments. We successfully tested our predictions in both synthetic and real systems. Finally, from finite-size scaling analysis we showed that the critical behavior of both S and χ in the abrupt region exhibits the features of a genuine first-order phase transition.

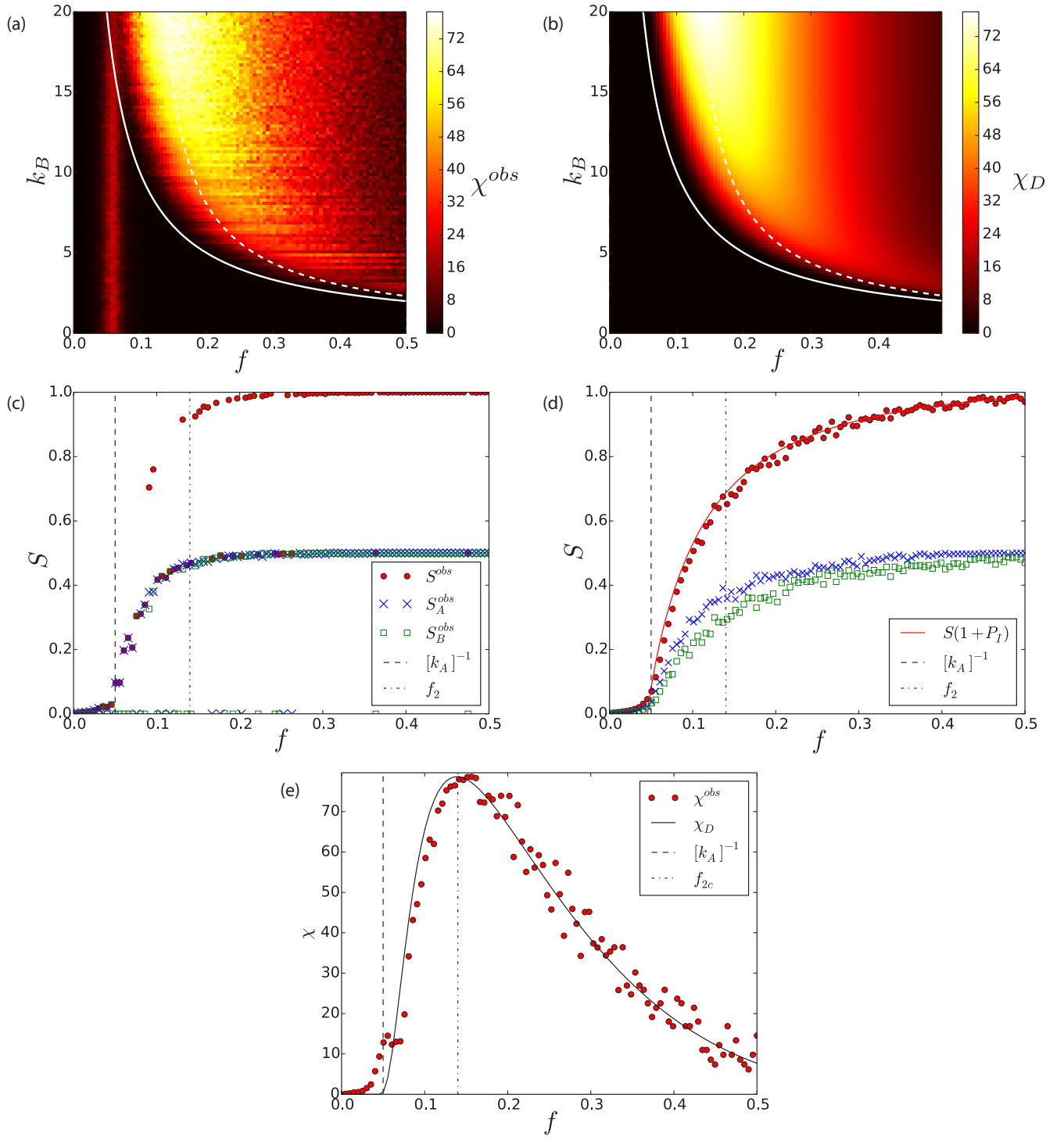

FIG. 3. Susceptibility and order parameter of weakly interacting Erdős-Rényi networks. We use $N_A = N_B = 500$ nodes, $k_A = 20$, $I = 5$, and k_B varying from 0 to k_A. (a) The susceptibility χ obtained from numerical simulations of the percolation process; (b) χ_D from numerical solutions of Eq. (3). In both panels the continuous white line gives the relation $f = k_B^{-1}$ that marks the boundary for the region in which percolating clusters exist in both layers, and the dashed white line shows values of f_2 as given by Eq. (4). The vertical strip in panel (a) for $f_1 = k_A^{-1}$ corresponds to the peak of χ_C (the susceptibility of layer A), which is not captured by χ_D. Panels (c)–(e) report the behavior of susceptibility and giant component size for the degenerate case $k_A = k_B = 20$. In all three cases, the dashed vertical line denotes f_1, the percolation threshold of the individual layers, whereas the dashed-dotted line denotes f_2 as derived from Eq. (5). The size of the giant component (i.e., the order parameter) is reported in panel (c) for individual realizations of the process and in panel (d) as an average over 300 realizations. In both panels full red dots are the observed values of S, while blue crosses and green squares are the observed values of S_A and S_B, respectively, and the continuous red line gives the numerical estimate of $\langle S \rangle$ derived from Eq. (2). (e) The observed susceptibility χ (full red dots) averaged over 300 realizations, as well as the numerical value of χ_D (continuous black line).

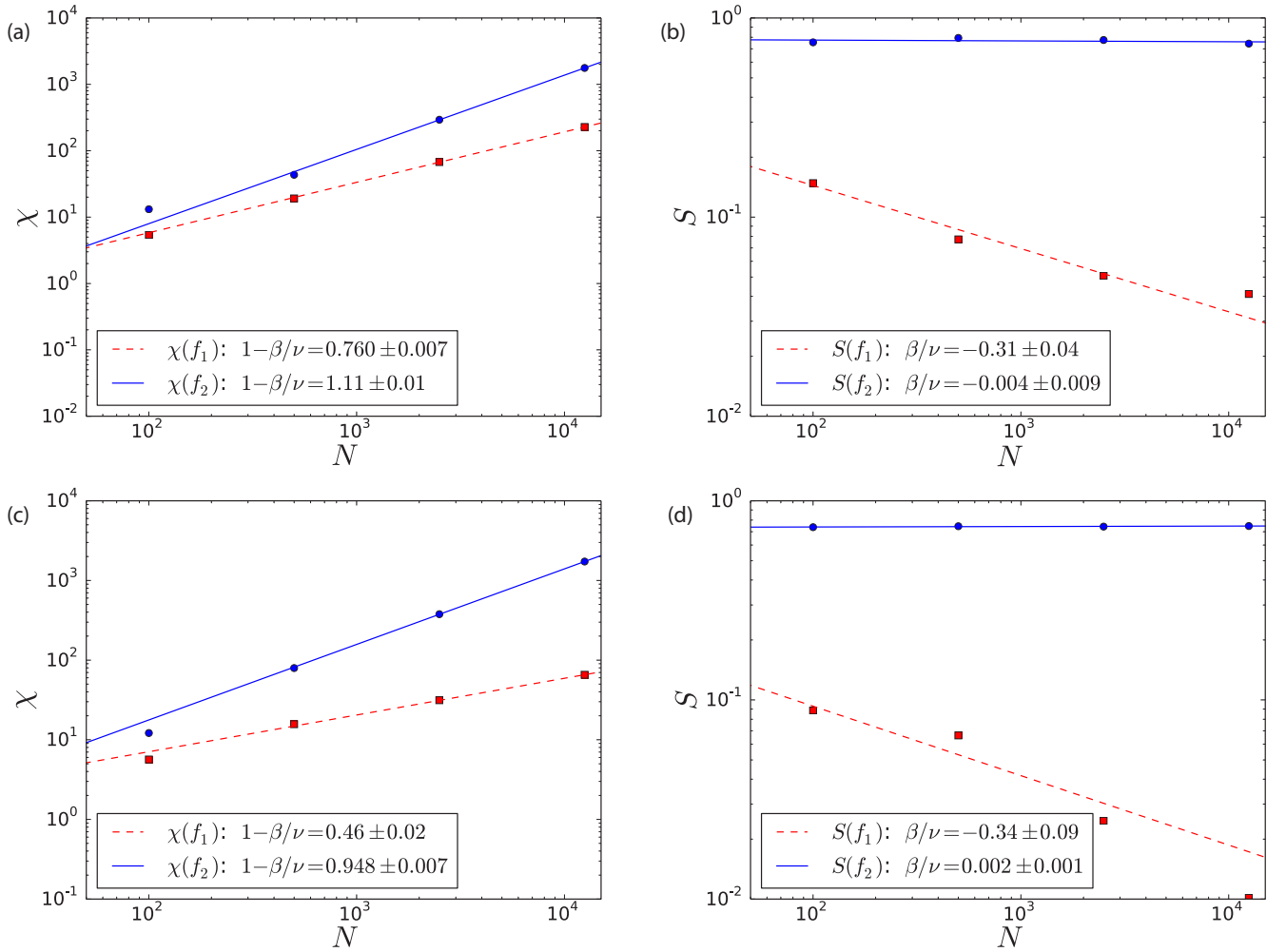

FIG. 4. Finite-size scaling analysis, reporting the divergence of susceptibility $\chi(f_c) \sim N^{1-\beta/\nu}$ and giant component size $S(f_c) \sim N^{-\beta/\nu}$ around the two critical values of f_c: f_1 for the standard continuous percolation transition of layer A, and f_2 for the discontinuous transition due to the merger of the giant clusters of the two layers (i.e., the value that maximizes χ_D). The top panels (a, b) report the case of two weakly interacting Erdős-Rényi layers with $k_A = 20$, $k_B = 10$, and $I = 5$, for different size N. From panel (b) we see that while $S(f_1)$ shows a power law decay with exponent $\beta/\nu = 0.31 \pm 0.04$ (which is consistent with the mean-field values $\beta = 1$ and $\nu = 3$), $S(f_2)$ does not scale with N. Accordingly to those values, from panel (a) we can verify the different divergence rates for the two peaks of the susceptibility, and in particular we see that the divergence of $\chi(f_2)$ is almost linear. The bottom panels (c, d) report the case of two weakly interacting Barabási-Albert layers with $m_A = 20$, $m_B = 10$, and $I = 5$, for different size N. Again we see that while $S(f_1)$ and $\chi(f_1)$ show a scaling behavior ruled by the topology of the layers, $S(f_2)$ and $\chi(f_2)$ show the same behavior of the Erdős-Rényi case: the one characteristic of first-order phase transitions.

Our work can have important applications in characterizing the fragility of weakly interacting structures such as multiplex transportation networks, as well as in describing epidemic processes on networks with metapopulation structures [29–33]. Additionally, our study highlights that fluctuations in finite systems must not always be treated as deviations from the thermodynamic limit due to finite-size effects [34]. Rather, they can carry important information on the system, and thus have to be taken into account especially when studying real-world networks [35].

At the time of submission of this paper, we became aware of a very recent publication [36], whose content is related to ours. In this work, the authors brilliantly address the problem of large fluctuations in the response of real multiplex networks to random node failures. Both this and our approaches are complementary and should play an important role in the theory of resilience of multilayer structures.

ACKNOWLEDGMENTS

A.A. acknowledges the Spanish MINECO (Grant no. FIS2015-71582-C2-1) and funding from ICREA Academia and the James S. McDonnell Foundation. G. Caldarelli and G. Cimini acknowledge support from the EU H2020 projects DOLFINS (Grant no. 640772) and CoeGSS (Grant no. 676547).

APPENDIX

In order to derive the analytic approximations presented in both Eqs. (4) and (5) in the case of two Erdős-Rényi layers of the same size ($N_A = N_B = N/2$), we start from the implicit

form of S_A and S_B in the thermodynamic limit:

$$S_X = \tfrac{1}{2}(1 - e^{-2fk_X S_X}) \tag{A1}$$

with $X = \{A, B\}$. The above expression is obtained from the usual equation for a single Erdős-Rényi network, namely, $S = 1 - e^{-fkS}$, using the substitution $S \to 2S$ (as S_X refers to only one layer with half of the N nodes). We thus obtain the same solution of the single network scaled by a factor $1/2$, as well as the same percolation threshold $f_X = k_X^{-1}$. The value of f which maximizes χ_D of Eq. (3) for fixed S_A and S_B is given by the following implicit equation:

$$[1 - 4f_2 S_A S_B]^I = 1 + \frac{S_A - \sqrt{S_A^2 + S_A S_B}}{S_B}, \tag{A2}$$

where both S_A and S_B are functions of f_2 according to Eq. (A1). Note that Eq. (A2) returns $f_2 = 1 - (2 - \sqrt{2})^{1/I}$ in the limit $S_{A,B} \to 1/2$. This regime corresponds to the case $I \ll k_{A,B}$, for which we can safely assume that both layers have fully percolated before at least one interconnection link is activated, leading to a value of f_2 which does not depend on k_A or k_B. Since Eq. (A2) is difficult to handle, we can approximate f_2 with the value that maximizes $\mathrm{Var}(S)$ instead of χ_D. For a Bernoulli trial we simply have $P_I(f_2) = 1/2$, implying $f_2 = [1 - 2^{-1/I}]/[4S_A S_B]$. With the further assumption $S_A = 1/2$ (hence when layer A has already percolated) we have $f_2 = [1 - 2^{-1/I}]/[2S_B]$. Using Eq. (A1) we finally get the analytic solution presented in Eq. (4):

$$f_2 = \frac{1 - 2^{-1/I}}{1 - \exp[-k_B(1 - 2^{-1/I})]}.$$

In the limit $S_B \to 1/2$ this expression simplifies to $f_2 = 1 - 2^{-1/I}$, which is very close to the value that maximizes χ_D in the same regime.

In the degenerate case $k_A = k_B = k$, we have $S_A = S_B = S_X$, which leads to the simpler expressions:

$$\langle S \rangle = S_X(1 + P_I), \quad \chi_D = N\frac{S_X P_I(1 - P_I)}{1 + P_I}, \tag{A3}$$

and thus the value of f which maximizes χ_D at fixed S_X is given by the implicit expression $P_I(f_2) = \sqrt{2} - 1$, implying $f_2 = [1 - (2 - \sqrt{2})^{1/I}]/[4S^2]$. Plugging the latter in Eq. (A1) yields Eq. (5):

$$f_2 = \frac{1 - (2 - \sqrt{2})^{1/I}}{(1 - \exp\{-k\sqrt{f_2[1 - (2 - \sqrt{2})^{1/I}]}\})^2}.$$

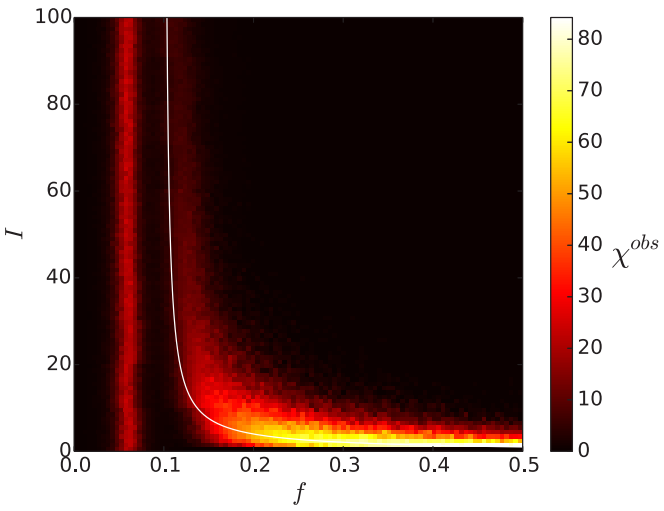

FIG. 5. Heat map of the susceptibility χ for two strongly connected Erdős-Rényi layers of $N = 500$ with $k_A = 20$, $k_B = 10$, and $0 < I < 100$. For every fixed value of I, χ is averaged over 400 realizations of the bond percolation process. The continuous white line represents the theoretical prediction from Eq. (4), which for large values of I converges to $k_B^{-1} = 0.1$.

We finally consider the case of strongly interacting Erdős-Rényi layers, which we define by $I \geqslant \max\{k_A, k_B\}$. As shown in Fig. 5 (where $k_A > k_B$), as soon as $I > k_A$ the height of the second peak drastically decreases, while the corresponding value of f_2 approaches k_B^{-1}, that is, the percolation threshold of the weak layer. The fact that $f_2 \to k_B^{-1}$ is obtained by taking the limit $I^{-1} \to 0$ in Eq. (4). Indeed, in this regime $P_I \simeq 1$ as soon as the percolating cluster appears in layer B: the process bears no uncertainty related to the interconnections, therefore contribution of χ_D vanishes and χ simply becomes that of the ordinary percolation process for the Erdős-Rényi layer B.

[1] D. Stauffer and A. Aharony, *Introduction to Percolation Theory*, 2nd rev. ed. (CRC Press, Boca Raton, FL, 2014).

[2] S. N. Dorogovtsev, A. V. Goltsev, and J. F. F. Mendes, Rev. Mod. Phys. **80**, 1275 (2008).

[3] D. S. Callaway, M. E. J. Newman, S. H. Strogatz, and D. J. Watts, Phys. Rev. Lett. **85**, 5468 (2000).

[4] M. E. J. Newman, S. H. Strogatz, and D. J. Watts, Phys. Rev. E **64**, 026118 (2001).

[5] F. Radicchi and C. Castellano, Nat. Commun. **6**, 10196 (2015).

[6] R. Cohen, D. ben-Avraham, and S. Havlin, Phys. Rev. E **66**, 036113 (2002).

[7] C. Castellano and R. Pastor-Satorras, Phys. Rev. Lett. **105**, 218701 (2010).

[8] S. V. Buldyrev, R. Parshani, G. Paul, H. E. Stanley, and S. Havlin, Nature (London) **464**, 1025 (2010).

[9] S.-W. Son, G. Bizhani, C. Christensen, P. Grassberger, and M. Paczuski, Europhys. Lett. **97**, 16006 (2012).

[10] G. J. Baxter, S. N. Dorogovtsev, A. V. Goltsev, and J. F. F. Mendes, Phys. Rev. Lett. **109**, 248701 (2012).

[11] E. A. Leicht and R. M. D'Souza, arXiv:0907.0894.

[12] S. Shai, D. Y. Kenett, Y. N. Kenett, M. Faust, S. Dobson, and S. Havlin, Phys. Rev. E **92**, 062805 (2015).

[13] B. Requião da Cunha, J. C. González-Avella, and S. Gonçalves, PLoS ONE **10**, e0142824 (2015).

[14] F. C. Hoppensteadt and E. M. Izhikevich, *Weakly Connected Neural Networks* (Springer-Verlag, New York, NY, USA, 1997).

[15] M. Dickison, S. Havlin, and H. E. Stanley, Phys. Rev. E **85**, 066109 (2012).
[16] S. Melnik, M. A. Porter, P. J. Mucha, and J. P. Gleeson, Chaos **24**, 023106 (2014).
[17] P. Colomer-de-Simón and M. Boguñá, Phys. Rev. X **4**, 041020 (2014).
[18] A. Faqeeh, S. Melnik, P. Colomer-de-Simón, and J. P. Gleeson, Phys. Rev. E **93**, 062308 (2016).
[19] M. E. J. Newman and R. M. Ziff, Phys. Rev. Lett. **85**, 4104 (2000).
[20] E. J. Friedman and A. S. Landsberg, Phys. Rev. Lett. **103**, 255701 (2009).
[21] D. Achlioptas, R. M. D'Souza, and J. Spencer, Science **323**, 1453 (2009).
[22] P. Grassberger, C. Christensen, G. Bizhani, S.-W. Son, and M. Paczuski, Phys. Rev. Lett. **106**, 225701 (2011).
[23] J. Nagler, A. Levina, and M. Timme, Nat. Phys. **7**, 265 (2011).
[24] J. Nagler, T. Tiessen, and H. W. Gutch, Phys. Rev. X **2**, 031009 (2012).
[25] R. M. D'Souza and J. Nagler, Nat. Phys. **11**, 531 (2015).
[26] A. Cardillo, J. Gómez-Gardeñes, M. Zanin, M. Romance, D. Papo, F. d. Pozo, and S. Boccaletti, Sci. Rep. **3**, 1344 (2013).
[27] B. Karrer, M. E. J. Newman, and L. Zdeborová, Phys. Rev. Lett. **113**, 208702 (2014).
[28] F. Radicchi and S. Fortunato, Phys. Rev. Lett. **103**, 168701 (2009).
[29] Y. Wang and G. Xiao, Phys. Lett. A **376**, 2689 (2012).
[30] F. D. Sahneh, C. Scoglio, and F. N. Chowdhury, in *Conf. 2013 American Control Conf.* (IEEE, Washington, DC, 2013), pp. 2307–2312.
[31] J. Hindes, S. Singh, C. R. Myers, and D. J. Schneider, Phys. Rev. E **88**, 012809 (2013).
[32] B. Wang, G. Tanaka, H. Suzuki, and K. Aihara, Phys. Rev. E **90**, 032806 (2014).
[33] Z. Ruan, M. Tang, C. Gu, and J. Xu, Chaos **27**, 103104 (2017).
[34] T. Kalisky and R. Cohen, Phys. Rev. E **73**, 035101(R) (2006).
[35] L. Hébert-Dufresne and A. Allard, arXiv:1810.00735.
[36] F. Coghi, F. Radicchi, and G. Bianconi, Phys. Rev. E **98**, 062317 (2018).